COMMENTS ON BARYON TRANSITION FORM FACTORS

Christoph Hanhart [a], Maxim Mai [b,c], Ulf-G. Meißner [d,a,e]
Deborah Rönchen [a]

[a]Institute for Advanced Simulation (IAS-4), Forschungszentrum Jülich
Jülich, Germany
[b]Albert Einstein Center for Fundamental Physics
Institute for Theoretical Physics, University of Bern
Sidlerstrasse 5, 3012 Bern, Switzerland
[c]The George Washington University, Washington, DC 20052, USA
[d]Helmholtz-Institut für Strahlen- und Kernphysik
and Bethe Center for Theoretical Physics, Universität Bonn
53115 Bonn, Germany
[e]Peng Huanwu Collaborative Center for Research and Education
International Institute for Interdisciplinary and Frontiers
Beihang University, Beijing 100191, China

Received 15 January 2026, accepted 16 January 2026,
published online 10 February 2026

We discuss in rather general terms the properties of space-like baryon transition form factors. In particular, we argue why these are necessarily complex-valued, what can be deduced from the respective phase motion, and why dealing with real-valued transition form factors in general leads to misleading results. For illustration, the transition form factors for the Roper resonance as derived in the Jülich–Bonn–Washington framework are discussed.

DOI:10.5506/APhysPolB.57.2-A17

1. Introduction

Physical states can appear either as bound states, virtual states or resonances. Bound states are stable systems, with normalized wave functions. Mathematically, they manifest themselves as poles of the S-matrix on the physical Riemann sheet. Examples for those poles, allowed only below the lowest threshold of the system, are the proton, the neutron (although the neutron can decay weakly, its lifetime is so long that it often can be treated as stable), and the deuteron as a bound system of proton and neutron. Virtual states and resonances are also connected to poles of the S-matrix, however, those are located on an unphysical Riemann sheet and their wave functions are not normalizable. The poles for virtual states are located on the real axis below the lowest threshold, those of resonances in the complex plane. Typically, both kinds of poles leave an imprint on observables. A famous virtual state is the neutron–neutron state, located only about 90 keV below threshold on the second sheet. Examples for resonances are the $\rho(770)$ meson and the $\Delta(1232)$ baryon — and the Roper resonance, $N^*(1440)$ [1].

A key question in hadron spectroscopy is the composition of states. The most simple realization of the quark model assigns baryons as three-quark states and mesons as quark–anti-quark systems. However, in recent years, it has become evident that QCD generates much more complicated structures, especially multi-quarks, where the quark content exceeds the numbers given above for the naive quark model. In the doubly heavy quark sector, the number of candidates for multi-quark states exceeds now that for regular quarkonia as soon as the energy is above the lowest open-flavor threshold; see Refs. [2–10] for recent reviews. In the light quark sector, *e.g.*, in the case of the $\Lambda(1405)$, there is a well established state that does not fit into a conventional classification [11, 12], it even reveals a two-pole structure. For dedicated reviews, see, *e.g.*, [13, 14]. The Roper resonance also shows unusual properties, see, *e.g.*, [15]. For example, it is lighter than the first negative parity excitation of the nucleon, the $S_{11}(1535)$, and the πN inelasticity drops very steeply right in the mass range of the Roper state. It is also the first baryon resonance which has a sizable decay rate into a three-particle final state with two pions, making it an important testbed for three-particle dynamics. Through this, the Roper resonance became also a long-term goal motivating a lot of *ab-initio* lattice QCD efforts in conducting calculations and improving the theoretical tool-box mapping finite-volume results to infinite-volume quantities [16–20]. Notable intermediate steps in this regard have recently been the first-ever calculations of 3-body resonances $\omega(782)$ [21] and the first excited state of pion $\pi(1300)$ [22] — a state 10 times heavier than its ground state, and nearly as heavy as the Roper resonance itself.

In resolving the structure and composition of resonant states, photons (real or virtual) provide a crucial scanning probe. Indeed, electro-magnetic transition form factors, to be introduced in Section 3, are believed to provide better insight into the structure of the exotic candidates. In the next section, we will first provide a quick review of the properties of resonances. For more details, we refer to the review “Resonances” in the «Review of Particle Physics» (RPP) [23] and references therein, as well as Refs. [24, 25].

2. On the properties of resonances

A resonance is characterized by its pole locations and its residues. Here, we wrote deliberately plural for both properties, since a resonance has poles on various Riemann sheets and, when it couples to various channels, also various residues (which are different for the different poles). However, the significance of a given resonance pole depends on its distance from the physical axis. Thus, in many cases, the observables are mostly influenced by a single pole and it is this single pole that is quoted in the RPP. For simplicity, this is the case we focus on from here on.

Let us assume a scattering amplitude contains a pole. Then it is always possible to split it according to

$$T(s)_{ij} = T(s)_{\mathrm{bg}\, ij} + T(s)_{\mathrm{R}\, ij}\,, \tag{1}$$

where the first term, $T(s)_{\mathrm{bg}}$ is regular at $s = s_{\mathrm{R}}$, and the second term, $T(s)_{\mathrm{R}}$ has a pole at that location. The indices i and j specify the pertinent channels, in the case of the Roper resonance discussed below, those are πN and $\pi\pi N$ (typically parameterized as ρN, σN, and $\pi\Delta$). The pole location s_{R} should, in principle, carry a label of the sheet where the pole is located, which we omit here to simplify notations.

Note that the decomposition provided in Eq. (1) is not unique. Especially for real values of s, one can straightforwardly shift strength from one term to the other. The only way to define resonance properties unambiguously and independently of a particular reaction is through an analytic continuation of the physical amplitude to the resonance pole s_{R} and then to extract the pole residues.

In this section, we follow Ref. [26] and discuss a special form of the decomposition given in Eq. (1). In particular, we assume that the background is diagonal in the channel-space, although in general this is not the case, and is constructed in a unitary way. Since the full T-matrix is unitary as well, T_{R} cannot be unitary individually. Instead, it takes the form (although we discuss predominantly baryons in this note, we refrain from keeping track with the Dirac structure to simplify notations) [27, 28]

$$T_{\mathrm{R}\, ij} = -\Gamma(s)^{\dagger}_{\mathrm{out}\, k}\delta_{ki}\frac{g_i n_i(s) n_j(s) g_j}{s - m^2 - \sum_a g_a^2 \Sigma(s)_a}\delta_{jl}\Gamma(s)_{\mathrm{in}\, l}\,, \tag{2}$$

with

$$\begin{aligned}
\mathrm{Disc}\left[\Gamma(s)^{\dagger}_{\mathrm{out}\ k}\right] &= 2i\ T(s)^{*}_{\mathrm{bg}\, kk}\,\rho_k(s)\,\Gamma(s)^{\dagger}_{\mathrm{out}\, k}\,, &(3)\\
\mathrm{Disc}\left[\Gamma(s)_{\mathrm{in}\ k}\right] &= 2i\ \Gamma(s)_{\mathrm{in}\, k}\,\rho_k(s)\,T(s)^{*}_{\mathrm{bg}\, kk}\,, &(4)\\
\mathrm{Disc}\left[\Sigma(s)_k\right] &= 2i\ \Gamma(s)_{\mathrm{in}\, k}\rho_k(s) n_k(s)^2 \Gamma(s)^{\dagger}_{\mathrm{out}\, k}\,, &(5)
\end{aligned}$$

where $\rho_k(s) = q_k/(8\pi\sqrt{s})$ and $n_k(s) = (q_k/q_0)^{\ell_k} F(q_k/q_0)_{\ell_k}$ denote the phase-space factor and the centrifugal barrier factor with respect to the channel-specific angular momentum ℓ_k, respectively. The function F_ℓ denotes phenomenological form factors necessary to tame the otherwise unlimited growth of the centrifugal barrier term for $\ell_k > 0$. One typically chooses [29–31]

$$F(z)_0^2 = 1\,, \qquad F(z)_1^2 = \left(1+z^2\right)^{-1}\,, \qquad F(z)_2^2 = \left(9+3z^2+z^4\right)^{-1}\,, \quad \ldots \tag{6}$$

A minimal resonance model, with $T_{\rm bg} = 0$, in a single channel reaction is characterized by two parameters, the bare mass and the bare coupling[1]. These can be employed to exactly reproduce the real and imaginary parts of the most significant pole location of a resonance. In this way, the residue is fixed automatically as well. In Ref. [26], it is demonstrated that in this way the residue of the ρ meson is described well. In contrast to this, a proper description of the $f_0(500)$ residue was possible only when a background was included. Interestingly, this background, when adjusted to reproduce both the absolute value of the residue and its phase, automatically introduced an Adler zero to the scattering amplitude as demanded by chiral symmetry, nicely showing the intimate relation between the properties of the $f_0(500)$ and chiral symmetry. The way the background modifies the vertex function is illustrated in Fig. 1. In particular, there are phases from both the background T-matrix as well as the intermediate two-particle state.

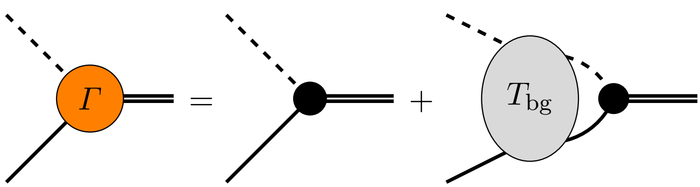

Fig. 1. Diagrammatic representation of the vertex function $\pi N \to R$, denoting nucleon/pion/resonance states by a full/dashed/double line, respectively. The full vertex function (Γ) is given by the sum of the bare vertex ($\bullet$) plus a contribution, where the external particles interact via the background interaction ($T_{\rm bg}$), shown as the gray ellipse.

The above-mentioned differences between the ρ and the σ amplitude can be interpreted such that the ρ has a conventional $\bar{q}q$ structure, while the $f_0(500)$ owes its existence to non-perturbative $\pi\pi$ interactions — this conclusion is in line with other, independent studies; see Ref. [32] for a review. This important information is encoded in both the pole residue and the

[1] Note that these bare quantities are devoid of any physical meaning.

phase. It is obvious that also the transition form factor is sensitive to the internal structure of a given state. Even more so, since the virtuality of the photon provides an additional degree of freedom. This is discussed in the next section.

3. Transition form factors

As discussed in the previous section also for transition from factors (TFFs), only resonance properties at the pole are well defined and, accordingly, also transition form factors should be extracted at the resonance pole. To find the proper theoretical expressions, the vertex function $\Gamma_{\rm in}$ that appears in $T_{\rm R}$, provided in Eq. (2), needs to be gauged. For a generic procedure in the context of Effective Field Theories, see, *e.g.*, Refs. [33–37]. In this way, the information about the presence or absence of a background term also gets transferred to the transition form factor. In particular, the transition form factor is necessarily complex-valued, although the photon is typically spacelike, such that crucial information is encoded in the emerging phase. Since the two-particle intermediate state, shown explicitly in the diagram on the far right of Fig. 2, can typically go on-shell for a resonance, which has open decay channels, there is an unavoidable non-trivial phase motion for all these resonances, where the presence of background terms are crucial (see discussion in the previous section) even at the pole.

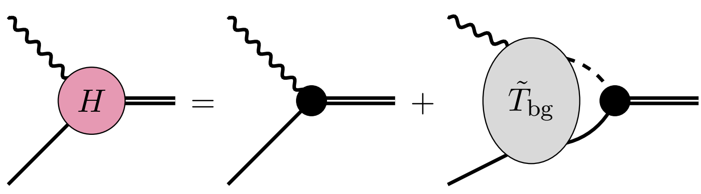

Fig. 2. Diagrammatic representation of the transition form factor H, denoting nucleon/photon/resonance states by a full/wavy/double line, respectively. The full form factor is given by the sum of the bare vertex (•) plus a contribution, where the external particles interact via the background interaction $\tilde{T}_{\rm bg}$, shown as the gray ellipse.

It is important to stress that since pole and non-pole contributions cannot be separated model-independently as stated above, it is also not possible to model-independently disentangle the so-called meson cloud contributions to the transition form factor and pure resonance contributions, see also the discussion in [38]. However, it follows from the discussion in the previous paragraph that if the phases of the hadronic residues differ significantly from those of the transition form factors, there must be background contributions present pointing at a non-trivial structure of the resonance.

The electromagnetic TFFs of a stable state (*e.g.*, N) to an excited state (*e.g.*, $N^*(1440)$) cannot be measured directly, since the resonance is not an asymptotically stable state but decays, for example, into πN or $\pi\pi N$ final states. TFFs, therefore, need to be extracted from electroproduction amplitudes, *e.g.*, for $\gamma^* N \to \pi N$, constrained by experimental data from, *e.g.*, CLAS@JLAB [39–42]. In the following, we show a possible procedure for the extraction of TFFs from experimental electroproduction data.

First, we note that any electroproduction observable to a two-body final state is a function of five independent kinematic variables. One useful choice of those is depicted in Fig. 3. The transition of successively separating off the angular dependence is visualized in the bottom part of Fig. 3, leaving one with electric, magnetic, and longitudinal multipoles $\{\mathcal{M}_{\ell\pm}(W,Q^2)|\mathcal{M} = E, M, L\}$. Here, $W = \sqrt{s}$, $Q^2 := -q^2$, and ℓ denote total energy, photon virtuality, and the relative angular momentum of the pion–nucleon pair, respectively. The total angular momentum $J = \ell \pm 1/2$ is specified via $\ell\pm$ (for final meson states with non-vanishing spin, the notation needs to be generalized). Different coupled-channel models (*e.g.*, MAID [46], ANL/Osaka [47], JBW [43], see also recent dedicated review [48]) can be compared conveniently on the level of these in general complex-valued multipoles. For example, in the JBW approach (see Fig. 4 for a visualization), which we take here as an example, the multipoles are parametrized as

$$\mathcal{M}_{\ell\pm} = V^{\gamma^*}_{\ell\pm} + \int_0^\infty \mathrm{d}p\, p^2\, T_{\ell\pm} G V^{\gamma^*}_{\ell\pm}\,, \tag{7}$$

where we have suppressed channel and isospin indices of the coupled-channel problem as well as all kinematic variables to ease the notation. Note also that an additional factorization of $V^{\gamma^*}_{\ell\pm}$ has been undertaken in the original JBW formulation. A complete set of formulas can be found in Refs. [43–45]. In the coupled-channel space, the elements denote:

— V^{γ^*}: photon-induced meson–baryon production potential;

— $T_{\ell\pm}$: coupled-channel meson–baryon scattering amplitude (constrained/fixed in purely hadronic reactions);

— G: meson–baryon Green's function (fixed by the formalism);

The meson–baryon scattering amplitude is itself a solution of a Lippmann–Schwinger coupled-channel equation

$$T_{\ell\pm} = V_{\ell\pm} + \int_0^\infty \mathrm{d}p\, p^2\, V_{\ell\pm} G T_{\ell\pm}\,. \tag{8}$$

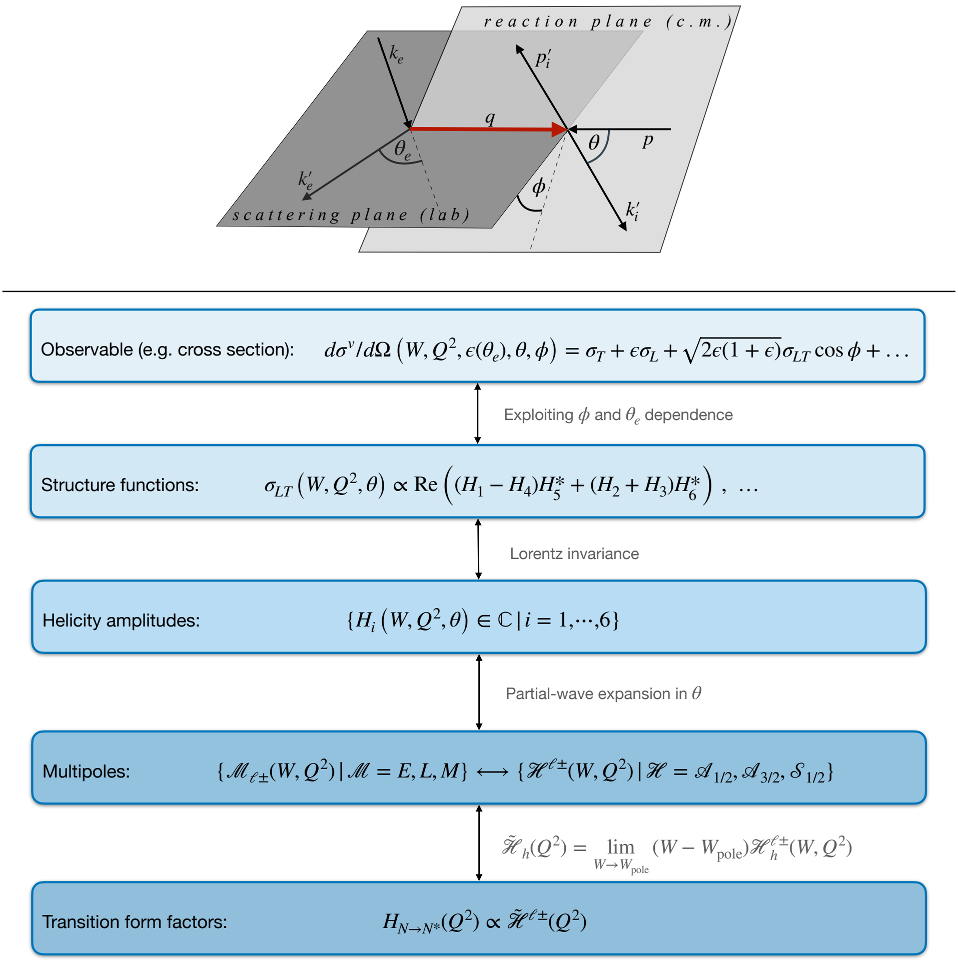

Fig. 3. Top panel: Degrees of freedom of a one-meson electroproduction reaction. Bottom panel: Connection between reaction-independent transition form factors $H_{N\to N^*}$ and observables. For more details and formulas, see Refs. [43–45].

The scattering potential V is derived from a chiral-symmetric Lagrangian and includes s-channel processes accounting for genuine resonances, as well as t- and u-channel exchanges of mesons and baryons, respectively, and contact diagrams. This separation is depicted in Fig. 4. Note also that certain resonances are dynamically generated in this approach. Accordingly, the photon-vertex separates as (again suppressing most of the dependencies on kinematic variables)

$$V_{\ell\pm}^{\gamma^*} = F^{NP}(Q^2)\alpha^{NP} + F^{P}(Q^2)\frac{\gamma_{R\to MB}\gamma_{\gamma^* N\to R}}{W - m_{\rm b}}\,, \tag{9}$$

where the resonance bare mass ($m_{\rm b}$) and its bare couplings to the pertinent outgoing meson–baryon pair ($\gamma_{R\to MB}$) are fixed from the same Lagrangian as the hadronic scattering potential shown in Eq. (8), while the bare couplings to the incoming γN ($\gamma_{\gamma^* N\to R}$) are parameterized by polynomials. The same applies to the quantity α^{NP} that simulates the interaction of the photon with the background. The channel-(in)dependent form-factors $F^{NP}(F^{P})$ parametrize the sole photon-virtuality dependence of the potential. Constraints ensuring Siegert's condition are implemented, while the approach also respects final-state unitarity and gauge invariance by construction.

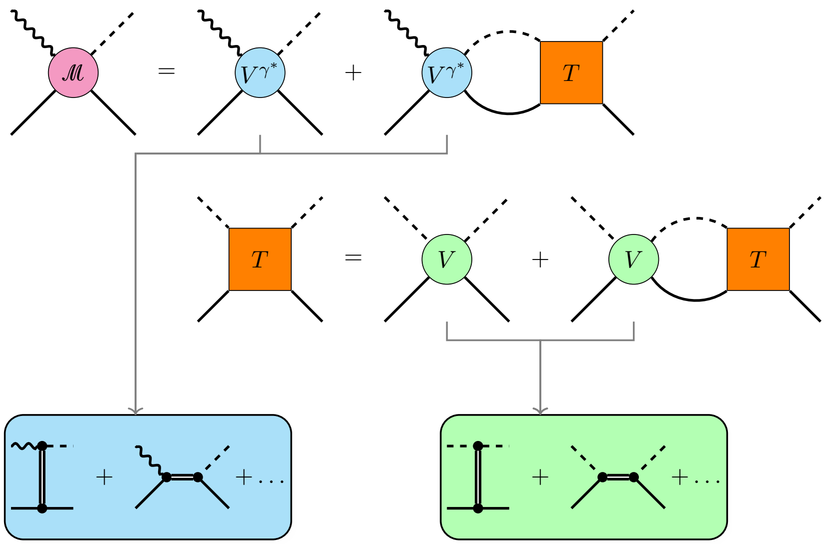

Fig. 4. JBW multipole parametrization. For any fixed quantum number, the multiples $\{\mathcal{M}_{\ell\pm}(W,Q^2)|\mathcal{M}=E,M,L\}$ are determined through a set of coupled-channel integral equations with respect to the scattering potential V and the electroproduction term V^{γ^*}.

The above procedure contains a set of free parameters determined from fits to the experimental data on elastic ($\pi N\to\pi N$) and inelastic ($\pi N\to \eta N, K\Lambda, K\Sigma$) πN reactions [49] as well as various reactions induced by real ($\gamma p\to\pi N,\eta N,K\Lambda$ [50]) and virtual photons ($\gamma^* p\to\pi N,\eta N,K\Lambda$ [43–45]) counting overall 8k+40k+110k = 158k data. The obtained multipoles $\mathcal{M}_{\ell\pm}$ can be accessed through the dedicated JBW-homepage [https://jbw.phys.gwu.edu].

Experimental observables are measured for real values of W. To access the transition form factors from the multipoles extracted in the procedure sketched above in a *reaction-independent* way, analyticity of both the multipoles as well as the scattering amplitude needs to be exploited for the (analytic) continuation to the resonance pole. Specifically, for any resonance (fixed total angular momentum J and isospin I) at the resonance pole ($W_{\rm pole}$), one can write

$$\mathcal{H} \propto \frac{\widetilde{\mathcal{H}}}{W - W_{\rm pole}} + \ldots\,, \qquad T \propto \frac{\widetilde{R}}{W - W_{\rm pole}} + \cdots\,, \tag{10}$$

where $\mathcal{H} \in \{\mathcal{A}_{\infty/\in}, \mathcal{A}_{\ni/\in}, \mathcal{S}_{\infty/\in}\}$ denotes a linear combination of the corresponding multipoles $\mathcal{M}$. Following Ref. [51] (see also Refs. [52, 53]), the transition form factors are then defined as

$$H\left(Q^2\right) = C_I \sqrt{\frac{p_{\pi N}}{\omega_0} \frac{2\pi(2J+1)W_{\rm pole}}{m_N \widetilde{R}}}\, \widetilde{\mathcal{H}}\left(Q^2\right)\,, \tag{11}$$

where $H \in \{A_{1/2}, A_{3/2}, S_{1/2}\}$. Here, ω_0 is the energy of the photon at $Q^2 = 0$, m_N the nucleon mass, and the isospin factor [54] $C_{1/2} = -\sqrt{3}$ and $C_{3/2} = \sqrt{2/3}$. Since at the pole the residues factorize into a product of incoming and outgoing effective couplings, the factor $\sqrt{\widetilde{R}}$ in the denominator removes the effective coupling (including its phase) connected to the outgoing final state from the expression, leaving the reaction-independent information on the transition form factor.

Using the latest JBW solution which provides an adequate description of the experimental data (*e.g.*, $\chi^2_{\gamma^*}$/d.o.f. < 1.5) and the procedure outlined above, one obtains the transition form factor of the Roper resonance [55]. In the left panel of Fig. 5, we show four different solutions of the fits — for later use in Fig. 6, we show the corresponding absolute values and phases of the transition form factors. In the right panel of Fig. 5, we show the results of other studies for the transition form factors as well as the TFFs provided by the CLAS Collaboration — these should not be confused with data, since there is some procedure necessary to come from the measured data to the TFFs. Note that all the TFFs extracted using the JBW approach describe the data equally well — although they appear to be rather different individually. Moreover, they all show non-negligible imaginary parts. In contrast to this, the TFFs extracted by the CLAS Collaboration are real valued. Furthermore, the comparison of the left and right panels of Fig. 5 suggests that the theoretical uncertainties assigned to the extraction by CLAS seem to be underestimated.

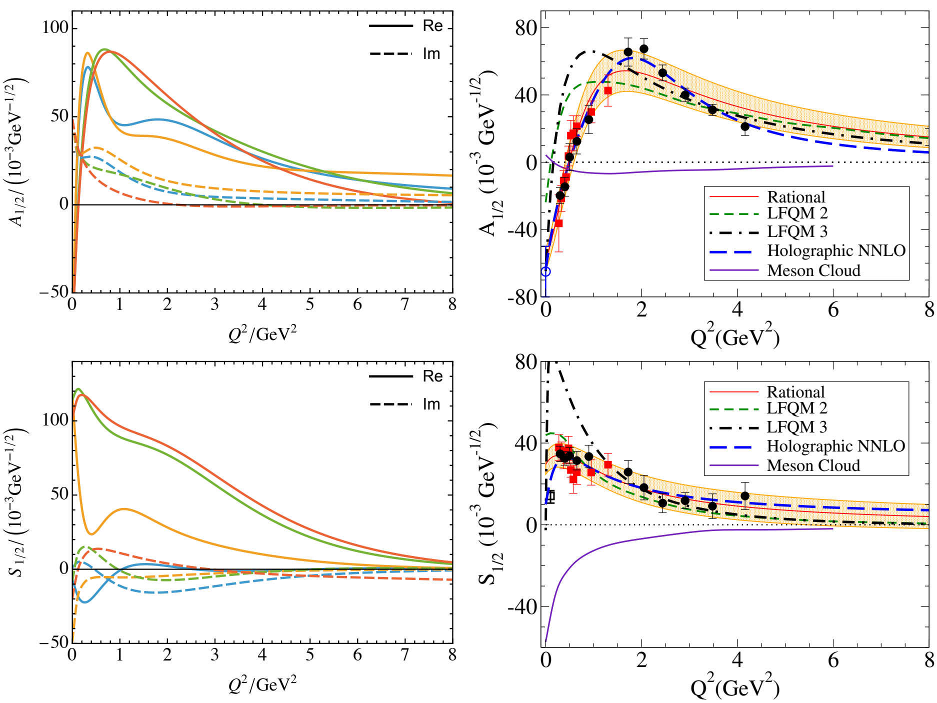

Fig. 5. Left panel: Representative results of the recent dynamical coupled-channel (JBW) approach. Right panel: overview of other approaches (adapted from a recent review [52]), employing strictly real transition form factors. The black and red data points show the extractions from the CLAS Collaboration for single [40] and double [42, 56] pion production, respectively.

The transition form factors provided by the CLAS Collaboration are extracted from the multipoles using the assumption that the resonances are well represented by the Breit–Wigner (BW) amplitudes with constant widths and real couplings to both the γN channel as well as the final states — for a comparison of the different extractions, see Ref. [51]. A comparison of the left and right panels of Fig. 5, thus, suggests that not only are the theoretical uncertainties severely underestimated, but also the assumption that the Roper resonance can be described by a fixed mass BW function is not justified. This also puts into question the interpretations of CLAS TFFs for the Roper resonance provided in, *e.g.*, Ref. [57].

4. Discussion and summary

We discuss the results shown in Fig. 6. A first important observation is that the absolute value of none of the transition form factors shows zero, contrary to those of Refs. [40, 42, 56]. Accordingly, an interpretation of that zero as a signature of the node in the Roper wave function that appears necessarily, if the resonance is a radial excitation of the nucleon, is hard to justify. However, what can be read off of Fig. 6 is that there is a very non-trivial hadronic dynamics taking place reflected in a strong Q^2 dependence of both the magnitude and the phase of the transition form factors.

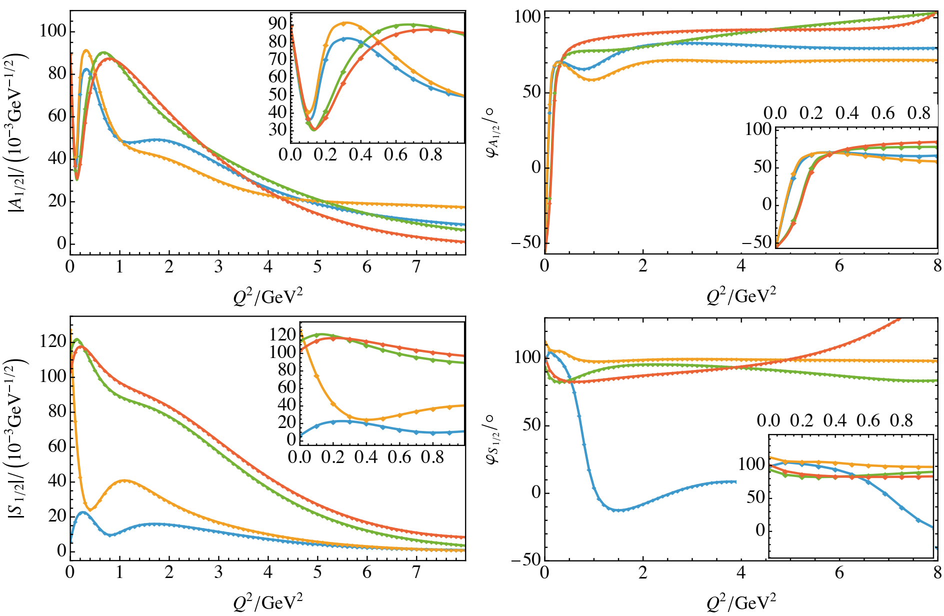

Fig. 6. Results of the recent dynamical coupled-channel (JBW) approach on transition form factors in terms of their absolute values (left) and phases (right).

The Jülich–Bonn–Washington dynamical coupled-channel model does not have any explicit pole term for the Roper resonance which appears to be generated dynamically from the meson-exchange potential through the scattering equation [15]. Given what has been said above, this description appears to be consistent with the available data. This observation raises a reasonable doubt on the claim that the meson cloud effects are negligible for the $A_{1/2}$ transition amplitude (see purple line in the upper right panel of Fig. 5). This is yet another important point questioning the interpretation of the CLAS TFFs provided in, *e.g.*, Ref. [57].

To summarize, transition form factors and couplings of resonances can be defined unambiguously only at the resonance poles[2]. Here, they typically develop non-trivial phases that should not be neglected. Applied to the case of the Roper resonance, we demonstrated that:

(a) From the presently available data, the transition form factors, especially $S_{1/2}$, cannot be extracted with high accuracy.

(b) There is a very strong energy dependence in the phase especially of $A_{1/2}$ pointing at meson–baryon dynamics being very relevant for the structure of this resonance.

In particular, the latter observation challenges the validity of the simple interpretation of the Roper resonance as the first radial excitation at least on the basis of the current experimental situation. Improved data should allow for an increased extraction accuracy for the electro-magnetic multipoles in the future. Crucially, however, also a sophisticated theoretical tool-box — based on a careful analytic continuation to the resonance poles — is necessary to uncover universal resonance properties from these data.

We are grateful to Gilberto Ramalho for very insightful discussions and for providing the figures in the right panels of Fig. 5. This work was funded in part by the Deutsche Forschungsgemeinschaft (DFG, German Research Foundation) as part of the CRC 1639 NuMeriQS — project No. 511713970, under Germany's Excellence Strategy — EXC 3107/1 — 533766364, by the European Research Council (ERC) under the European Union's Horizon 2020 research and innovation programme (grant agreement No. 101018170), by the MKW NRW under the funding code NW21-024-A, and by the CAS President's International Fellowship Initiative (PIFI) under grant Nos. 2025PD0022 (U.G.M.) and 2025PD0087 (C.H.). The work of M.M. was further funded through the Heisenberg Programme by the Deutsche Forschungsgemeinschaft (DFG, German Research Foundation) — 532635001. The numerical calculations were performed on JURECA-DC of the Jülich Supercomputing Centre, Jülich, Germany.

REFERENCES

[1] L.D. Roper, «Evidence for a P_{11} Pion–Nucleon Resonance at 556 MeV», *Phys. Rev. Lett.* **12**, 340 (1964).

[2] For a similar discussion of the Transition Generalized Parton Distributions exploring Baryon Resonances, see Ref. [58]

[2] A. Hosaka *et al.*, «Exotic hadrons with heavy flavors: X, Y, Z, and related states», *Prog. Theor. Exp. Phys.* **2016**, 062C01 (2016).

[3] A. Esposito, A. Pilloni, A.D. Polosa, «Multiquark resonances», *Phys. Rep.* **668**, 1 (2017).

[4] F.-K. Guo *et al.*, «Hadronic molecules», *Rev. Mod. Phys.* **90**, 015004 (2018); *Erratum ibid.* **94**, 029901 (2022).

[5] S.L. Olsen, T. Skwarnicki, D. Zieminska, «Nonstandard heavy mesons and baryons: Experimental evidence», *Rev. Mod. Phys.* **90**, 015003 (2018).

[6] M. Karliner, J.L. Rosner, T. Skwarnicki, «Multiquark States», *Annu. Rev. Nucl. Part. Sci.* **68**, 17 (2018).

[7] N. Brambilla *et al.*, «The XYZ states: Experimental and theoretical status and perspectives», *Phys. Rep.* **873**, 1 (2020).

[8] G. Yang, J. Ping, J. Segovia, «Tetra- and Penta-Quark Structures in the Constituent Quark Model», *Symmetry* **12**, 1869 (2020).

[9] H.-X. Chen *et al.*, «An updated review of the new hadron states», *Rep. Prog. Phys.* **86**, 026201 (2023).

[10] L. Meng, B. Wang, G.-J. Wang, S.-L. Zhu, «Chiral perturbation theory for heavy hadrons and chiral effective field theory for heavy hadronic molecules», *Phys. Rep.* **1019**, 1 (2023).

[11] N. Kaiser, P.B. Siegel, W. Weise, «Chiral dynamics and the low-energy kaon–nucleon interaction», *Nucl. Phys. A* **594**, 325 (1995).

[12] J.A. Oller, U.-G. Meißner, «Chiral dynamics in the presence of bound states: kaon–nucleon interactions revisited», *Phys. Lett. B* **500**, 263 (2001).

[13] M. Mai, «Review of the $\Lambda(1405)$ A curious case of a strangeness resonance», *Eur. Phys. J. Spec. Top.* **230**, 1593 (2021).

[14] T. Hyodo, M. Niiyama, «QCD and the strange baryon spectrum», *Prog. Part. Nucl. Phys.* **120**, 103868 (2021).

[15] O. Krehl, C. Hanhart, S. Krewald, J. Speth, «What is the structure of the Roper resonance?», *Phys. Rev. C* **62**, 025207 (2000).

[16] M.T. Hansen, S.R. Sharpe, «Relativistic, model-independent, three-particle quantization condition», *Phys. Rev. D* **90**, 116003 (2014).

[17] M. Mai, M. Döring, «Three-body unitarity in the finite volume», *Eur. Phys. J. A* **53**, 240 (2017).

[18] D. Severt, M. Mai, U.-G. Meißner, «Particle-dimer approach for the Roper resonance in a finite volume», *J. High Energy Phys.* **2023**, 100 (2023).

[19] M.T. Hansen, F. Romero-López, S.R. Sharpe, «Finite-volume formalism for $N\pi\pi$ at maximal isospin», arXiv:2509.24778 [hep-lat].

[20] S.R. Sharpe, «Three-particle scattering amplitudes from lattice QCD», arXiv:2601.04147 [hep-lat].

[21] H. Yan *et al.*, «ω Meson from Lattice QCD», *Phys. Rev. Lett.* **133**, 211906 (2024).

[22] H. Yan *et al.*, «Emergence of the $\pi(1300)$ Resonance from Lattice QCD», arXiv:2510.09476 [hep-lat].

[23] Particle Data Group (S. Navas *et al.*), «Review of Particle Physics», *Phys. Rev. D* **110**, 030001 (2024).

[24] M. Mai, U.-G. Meißner, C. Urbach, «Towards a theory of hadron resonances», *Phys. Rep.* **1001**, 1 (2023).

[25] S. Willenbrock, «Unstable Particles in Quantum Field Theory», arXiv:2511.16941 [hep-ph].

[26] L.A. Heuser *et al.*, «From pole parameters to line shapes and branching ratios», *Eur. Phys. J. C* **84**, 599 (2024).

[27] K. Nakano, «Two potental formalisms and the Coulomb-nuclear interference», *Phys. Rev. C* **26**, 1123 (1982).

[28] C. Hanhart, «A new parameterization for the pion vector form factor», *Phys. Lett. B* **715**, 170 (2012).

[29] J.M. Blatt, V.F. Weisskopf, «Theoretical Nuclear Physics», *Springer*, New York 1952.

[30] F. Von Hippel, C. Quigg, «Centrifugal-Barrier Effects in Resonance Partial Decay Widths, Shapes, and Production Amplitudes», *Phys. Rev. D* **5**, 624 (1972).

[31] S.U. Chung *et al.*, «Partial wave analysis in K-matrix formalism», *Ann. Phys.* **4**, 404 (1995).

[32] J.R. Peláez, «From controversy to precision on the sigma meson: A review on the status of the non-ordinary $f_0(500)$ resonance», *Phys. Rep.* **658**, 1 (2016).

[33] C.H.M. van Antwerpen, I.R. Afnan, «Gauge invariant unitary theory for pion photoproduction», *Phys. Rev. C* **52**, 554 (1995).

[34] B. Borasoy, P.C. Bruns, U.-G. Meißner, R. Nissler, «A gauge invariant chiral unitary framework for kaon photo- and electroproduction on the proton», *Eur. Phys. J. A* **34**, 161 (2007).

[35] D. Ruić, M. Mai, U.-G. Meißner, «η-Photoproduction in a gauge-invariant chiral unitary framework», *Phys. Lett. B* **704**, 659 (2011).

[36] M. Mai, P.C. Bruns, U.-G. Meißner, «Pion photoproduction off the proton in a gauge-invariant chiral unitary framework», *Phys. Rev. D* **86**, 094033 (2012).

[37] P.C. Bruns, «A formalism for the study of $K^+\pi\Sigma$ photoproduction in the $\Lambda^*(1405)$ region», arXiv:2012.11298 [nucl-th].

[38] V. Bernard, H.W. Fearing, T.R. Hemmert, U.-G. Meißner, «The form-factors of the nucleon at small momentum transfer», *Nucl. Phys. A* **635**, 121 (1998); *Erratum ibid.* **642**, 563 (1998).

[39] CLAS Collaboration (M. Ripani *et al.*), «Measurement of $ep \to e'p\pi^+\pi^-$ and Baryon Resonance Analysis», *Phys. Rev. Lett.* **91**, 022002 (2003).

[40] CLAS Collaboration (I.G. Aznauryan *et al.*), «Electroexcitation of nucleon resonances from CLAS data on single pion electroproduction», *Phys. Rev. C* **80**, 055203 (2009).

[41] CLAS Collaboration (V.I. Mokeev *et al.*), «Experimental Study of the $P_{11}(1440)$ and $D_{13}(1520)$ resonances from CLAS data on $ep \to e'\pi^+\pi^-p'$», *Phys. Rev. C* **86**, 035203 (2012).

[42] V.I. Mokeev *et al.*, «New results from the studies of the $N(1440)1/2^+$, $N(1520)3/2^-$, and $\Delta(1620)1/2^-$ resonances in exclusive $ep \to e'p'\pi^+\pi^-$ electroproduction with the CLAS detector», *Phys. Rev. C* **93**, 025206 (2016).

[43] Jülich–Bonn–Washington Collaboration (M. Mai *et al.*), «Jülich–Bonn–Washington model for pion electroproduction multipoles», *Phys. Rev. C* **103**, 065204 (2021).

[44] Jülich–Bonn–Washington Collaboration (M. Mai *et al.*), «Coupled-channels analysis of pion and η electroproduction within the Jülich–Bonn–Washington model», *Phys. Rev. C* **106**, 015201 (2022).

[45] Jülich–Bonn–Washington Collaboration (M. Mai *et al.*), «Inclusion of $K\Lambda$ electroproduction data in a coupled channel analysis», *Eur. Phys. J. A* **59**, 286 (2023).

[46] L. Tiator, «The MAID Legacy and Future», *Few-Body Syst.* **59**, 21 (2018).

[47] H. Kamano, «Electromagnetic N^* Transition Form Factors in the ANL-Osaka Dynamical Coupled-Channels Approach», *Few-Body Syst.* **59**, 24 (2018).

[48] M. Döring, J. Haidenbauer, M. Mai, T. Sato, «Dynamical coupled-channel models for hadron dynamics», *Prog. Part. Nucl. Phys.* **146**, 104213 (2026).

[49] D. Rönchen *et al.*, «Coupled-channel dynamics in the reactions $\pi N \to \pi N, \eta N, K\Lambda, K\Sigma$», *Eur. Phys. J. A* **49**, 44 (2013).

[50] D. Rönchen, M. Döring, U.-G. Meißner, «The impact of $K^+\Lambda$ photoproduction on the resonance spectrum», *Eur. Phys. J. A* **54**, 110 (2018).

[51] R.L. Workman, L. Tiator, A. Sarantsev, «Baryon photo-decay amplitudes at the pole», *Phys. Rev. C* **87**, 068201 (2013).

[52] G. Ramalho, M.T. Peña, «Electromagnetic transition form factors of baryon resonances», *Prog. Part. Nucl. Phys.* **136**, 104097 (2024).

[53] G. Ramalho, «Nucleon to Roper transition amplitudes and electromagnetic form factors», *Acta Phys. Pol. B* **57**, 2-A11 (2026), this issue, arXiv:2512.04493 [hep-ph].

[54] D. Drechsel, O. Hanstein, S.S. Kamalov, L. Tiator, «A unitary isobar model for pion photoproduction and electroproduction on the proton up to 1 GeV», *Nucl. Phys. A* **645**, 145 (1999).

[55] Jülich–Bonn–Washington Collaboration (Y.-F. Wang *et al.*), «Global Data-Driven Determination of Baryon Transition Form Factors», *Phys. Rev. Lett.* **133**, 101901 (2024).

[56] CLAS Collaboration (H. Denizli *et al.*), «Q^2 dependence of the $S_{11}(1535)$ photocoupling and evidence for a P-wave resonance in eta electroproduction», *Phys. Rev. C* **76**, 015204 (2007).

[57] V.D. Burkert, C.D. Roberts, «*Colloquium*: Roper resonance: Toward a solution to the fifty year puzzle», *Rev. Mod. Phys.* **91**, 011003 (2019).

[58] S. Diehl *et al.*, «Exploring baryon resonances with transition generalized parton distributions: status and perspectives», *Eur. Phys. J. A* **61**, 131 (2025).